Solid State Sciences 61 (2016) 220–224

Contents lists available at ScienceDirect

Solid State Sciences

journal homepage: www.elsevier.com/locate/ssscie

Pressure-induced transition to Ni_2In-type phase in lithium sulfide (Li_2S)

Oleg I. Barkalov [a, b, *], Pavel G. Naumov [a, c], Claudia Felser [a], Sergey A. Medvedev [a]

[a] Max-Planck-Institute for Chemical Physics of Solids, Nöthnitzer-Str. 49, Dresden, 01187, Germany
[b] Institute of Solid State Physics, Russian Academy of Sciences, Academician Ossipyan str. 2, Chernogolovka, Moscow District, 142432, Russia
[c] Shubnikov Institute of Crystallography of Federal Scientific Research Centre "Crystallography and Photonics" of Russian Academy of Sciences, Leninskii prospekt 59, Moscow, 119333, Russia

ARTICLE INFO

Article history:
Received 30 June 2016
Received in revised form
23 September 2016
Accepted 1 October 2016
Available online 3 October 2016

Keywords:
Chalcogenides
High pressure
Raman spectroscopy
X-ray diffraction
Crystal structure

ABSTRACT

Raman spectroscopy and synchrotron angle-dispersive X-ray diffraction were applied to investigate pressure-induced phase transitions in lithium sulfide (Li_2S). We observed two reversible transitions, first from the cubic antifluorite ($Fm\bar{3}m$) phase to an orthorhombic anticotunnite ($Pnma$) phase at about 13 GPa, followed by a transition to the hexagonal Ni_2In-type ($P6_3/mmc$) structure above 30 GPa, as previously predicted by *ab initio* density functional theory calculations.

1. Introduction

Systematic studies of pressure-induced phase transitions in compounds belonging to a particular family are important for understanding these transitions and their pathways, testing the applicability of theoretical models, and more generally, for understanding the properties of matter under extreme conditions.

The sequence of pressure-induced phase transitions for alkali metal sulfides (A_2S) has recently undergone investigation [1–5]. Li_2S, Na_2S, K_2S, and Rb_2S crystalize at ambient conditions in the cubic antifluorite structure (space group: $Fm\bar{3}m$). Under high pressure, Li_2S, Na_2S, and Rb_2S undergo an antifluorite-to-anticotunnite ($PbCl_2$-type structure with the space group: $Pnma$) phase transition at continuously lower pressures. Increasing the cation size [1,2,4] results in the stability of the anticotunnite structure of Cs_2S already at ambient pressure [5]. At higher pressures, a second phase transition from the anticotunnite phase to a hexagonal $P6_3/mmc$ Ni_2In-type phase (or its distorted analogue) was observed for Na_2S [2], Rb_2S [4], and Cs_2S [5], whereas in K_2S, the Ni_2In-type structure was identified at 6 GPa without the formation of the anticotunnite structure [3]. For Li_2S, a transition from the anticotunnite phase to a Ni_2In-type structure was predicted theoretically by *ab initio* total energy calculations in the pressure range 28.8–40.6 GPa, depending on the calculation method used [6,7]; however, it has not been observed experimentally until now.

It can be expected that the related family of alkali oxides (A_2O), which adopts the antifluorite structure at ambient conditions, will also follow the same series of phase transitions. Indeed, the only high-pressure studies of Li_2O reveal the antifluorite-to-anticotunnite phase transition at ~50 GPa [8,9].

Alkali metal chalcogenides and oxides are isoelectronic with ice (H_2O), for which a transition from symmetric ice X to the antifluorite structure of ice XI was predicted for pressures above 150 GPa [10,11]. Due to this similarity, an understanding of the high-pressure behavior of Li_2S will potentially aid in the description of dense ice structures that are important for planetary geosciences and fundamental chemistry. Investigation of this material will provide better understanding of more complex metal oxides and chalcogenides.

Recently, the transition to a superconducting state at high pressures was reported for H_2S at $T_c = 203$ K [12]. This critical

* Corresponding author. Institute of Solid State Physics, Russian Academy of Sciences, Academician Ossipyan str. 2, Chernogolovka, Moscow District, 142432, Russia.
E-mail addresses: barkalov@issp.ac.ru (O.I. Barkalov), pgnaumov@gmail.com (P.G. Naumov), Claudia.Felser@cpfs.mpg.de (C. Felser), Sergiy.Medvediev@cpfs.mpg.de (S.A. Medvedev).

http://dx.doi.org/10.1016/j.solidstatesciences.2016.10.002
1293-2558/

temperature is higher than that of any previously known superconducting compound and was attributed to the conventional mechanism of superconductivity caused by electron-phonon interaction, the high T_c arising due to the small mass of the hydrogen atom. However, an alternative explanation of the observed effect that implied the mechanism of hole superconductivity was proposed in Ref. [13]. Within the framework of this theory, insulating alkali metal sulfides (Li_2S, Na_2S, and K_2S) were proposed as candidates for high-temperature superconductivity at high pressure [13]. Phase transitions in these materials have thus far not been explored experimentally above 20 GPa. In order to clarify these theoretical propositions, the upper limit of the experimental studies should be raised to the Mbar pressure range.

In the present work, we report our results of the studies on phase transitions in Li_2S by *in situ* Raman spectroscopy and angle-dispersive X-ray diffraction in a diamond anvil cell up to 64 GPa at room temperature.

2. Material and methods

The finely powdered samples of Li_2S (Alfa-Aesar, nominal purity 99.98%) were loaded in a diamond anvil cell (DAC) with a stainless steel gasket. The diamond anvils had flat culets of 500 μm diameter. Because of the high sensitivity of Li_2S to oxygen and moisture, the sample batch was stored in a glovebox. The sample loading was performed in a glovebox in an atmosphere of pure argon, containing <0.1 ppm of oxygen and water. To avoid sample contamination, no pressure-transmitting medium was used.

In Raman spectroscopic measurements, a Melles Griot 25-LHP-928-230 HeNe laser with a nominal power of 35 mW was used for excitation, and the spectra were recorded in back-scattering geometry. The laser power at the sample position can be estimated as ≈26 mW because of losses due to the optical elements. Spectral acquisition was achieved using a customary Raman optical microscope system for DACs with a single imaging spectrograph (Princeton Instruments Acton SP 2500; focal length 500 mm), equipped with a diffraction grating of 1200 grooves/mm and a liquid nitrogen cooled charge-coupled device detector. The spectral resolution in the studied spectral range was of ~1 cm^{-1}. The Raman spectrometer was calibrated using Ne spectral lines with an error of ±1 cm^{-1}. The pressure was determined using the fluorescence lines of a ruby ball, which was loaded into the hole in the gasket in contact with the sample.

Angle-dispersive X-ray powder diffraction patterns were measured on the ID09A beamline at the European Synchrotron Radiation Facility using a monochromatic beam of wavelength λ = 0.41235 Å. The integration of two-dimensional images was done using the FIT2D program [14].

3. Results and discussion

At ambient pressure, Li_2S crystalizes in the cubic $Fm\bar{3}m$ antifluorite type structure. Symmetry analysis predicts only one Raman active mode of F_{2g} symmetry in this structure, corresponding to the breathing-type motion of the Li atom substructure. In this study, the Raman spectra recorded for Li_2S at pressures up to about 13 GPa show only this single peak (Figs. 1 and 2); X-ray diffraction patterns collected at low pressures can be unambiguously indexed to the antifluorite $Fm\bar{3}m$ structure (Figs. 3 and 4). The frequency of the observed Raman peak and its shift to higher frequencies upon compression (Fig. 2), as well as changes in the lattice parameters with increasing pressure (Fig. 5a), are in good agreement with data from previous high-pressure studies of Li_2S [1]. The fit of the third-order Birch-Murnaghan equation of state [15] to the experimental pressure-volume data (Fig. 5b) yields a bulk modulus (B_0) value of 52(4) GPa, in good agreement with previous experimental studies [1] and theoretical calculations [7].

At a pressure of ≈ 13 GPa, new bands in Raman spectra (Fig. 1) and additional peaks in the X-ray diffraction patterns (Fig. 3) appear, indicating a structural phase transition to the anticotunnite phase [1]. The observed Raman spectra and diffraction patterns indexed to the orthorhombic *Pnma* anticotunnite-type structure are in good agreement with previous studies [1], as are the pressure dependencies of the frequencies of Raman bands (Fig. 2) and lattice parameters (Fig. 5) [1]. The bulk modulus of Li_2S in the anticotunnite phase is found to be 133(3) GPa, which is very close to the

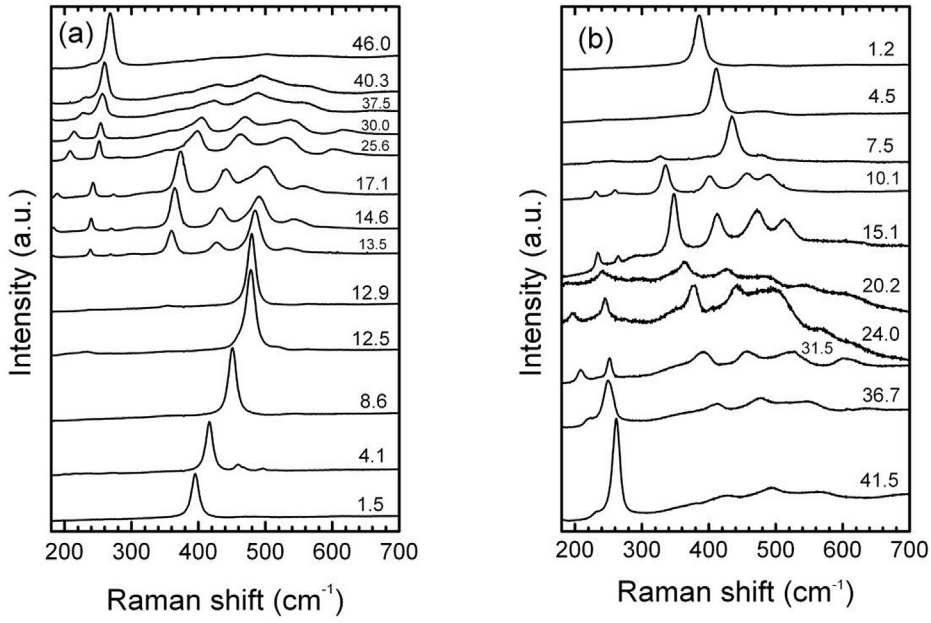

Fig. 1. Representative Raman spectra of Li_2S measured in the course of increasing (a) and decreasing pressure (b). Linear background presumably due to the luminescence from diamond anvils is subtracted from the spectra recorded at 51 and 64 GPa. Pressure values in GPa are given on the right hand side of the curves.

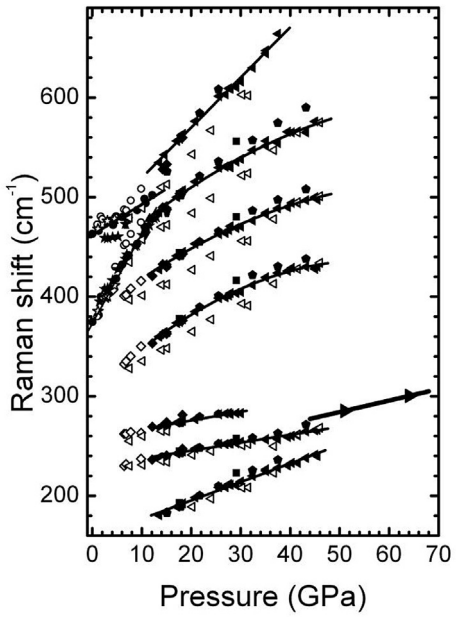

Fig. 2. The frequencies of the Raman active modes of Li_2S plotted as a function of pressure. Circles and diamonds refer to the data reported in Ref. [1] for cubic antifluorite and orthorhombic anticotunnite phases, respectively. Triangles, stars, pentagons and squares represent the data of the present work obtained in different pressure runs. Solid and open symbols are for increasing and decreasing pressure runs, respectively. Solid lines drown through the data points are the guides for eye.

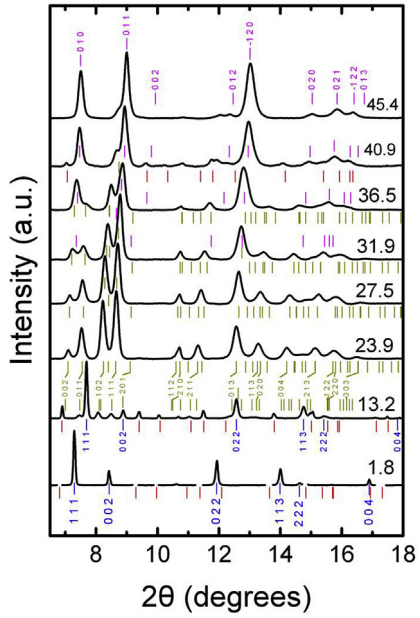

Fig. 3. X-ray powder diffraction patterns obtained upon increasing pressure. Red vertical bars denote reflections from the Al_2O_3 pressure gauge balls embedded in the Li_2S sample. Blue, dark yellow, and magenta vertical bars correspond to the Bragg reflections of low-pressure, cubic $Fm\bar{3}m$ phase, high pressure, orthorhombic *Pnma* phase and high pressure, hexagonal $P6_3/mmc$ phase (Ni_2In-type structure), respectively. Corresponding Miller indices are given below the bars. Digits to the right of each pattern denote the corresponding pressure values in GPa. Spurious reflections from Al_2O_3 were subtracted from the pattern obtained at 1.8 GPa. (For interpretation of the references to colour in this figure legend, the reader is referred to the web version of this article.)

previously reported value of 137 GPa [1]. The anticotunnite phase of Li_2S appears to be much less compressible when compared to its antifluorite structure. Similar behavior is also observed in Na_2S [2].

The anticotunnite structure appears to be stable up to a pressure of ≈ 30 GPa, above which changes in both Raman spectra and X-ray diffraction patterns indicate the onset of another structural phase transition. In Raman spectra, at pressure above 30 GPa, the intensity of the band located initially at a frequency near 250-260 cm^{-1} abruptly increases, whereas all other bands exhibit strong broadening and their intensities decrease. Finally, at pressures above 45 GPa, the mode with a frequency of 265 cm^{-1} appears to be the only spectral feature detected within the whole experimental frequency interval.

The X-ray diffraction patterns also reveal significant changes in the intensities of the peaks in the same pressure range (Fig. 3). For instance, the intensities of the diffraction peaks (002), (111), and (013) of the *Pnma* structure abruptly increase, whereas the intensity of the (102) peaks strongly decreases. The resulting diffraction patterns at pressures above 45 GPa can be assigned to the hexagonal lattice and the systematic absences are consistent with the $P6_3/mmc$ space group describing the Ni_2In-type structure, as shown in Figs. 3 and 4. A pressure-induced transition to this structure is expected to occur in Li_2S because the Ni_2In-type structure was previously observed at high pressures in all other alkali sulfides [2–5], and the anticotunnite-to-Ni_2In-type structure transition in Li_2S was theoretically predicted to occur in the pressure range from 28.8 to 40.6 GPa [6,7].

The diffraction pattern obtained at 45.4 GPa was used for Rietveld refinement (Fig. 4) using the program TOPAS 4.2 [16]. The refined parameters were Chebyshev polynomial background function, Stephens profile function [17] (to account for the anisotropic peak broadening due to a strain unavoidable for the case of the high-pressure experiments with an uniaxial compression component in a DAC [1]), cell parameters, and March-Dollase correction for preferred orientation. We obtained the following cell parameters for the $P6_3/mmc$ phase: a = 3.635(2) Å and c = 4.782(8) Å. Weak reflections near 11 and 12° (Fig. 4) that do not correspond to the Ni_2In-type high-pressure phase are presumably due to the remains of the *Pnma* phase.

The changes in Raman spectra are in agreement with structural transition to higher symmetry Ni_2In-type structure, and the only observed Raman band at 260 cm^{-1} can be assigned to the E_g-mode of the $P6_3/mmc$ structure. Unfortunately, no Raman spectroscopy data on the Ni_2In-type structure of other alkali sulfides have been reported, preventing any direct comparison with the spectra of the Li_2S high-pressure phase recorded in our study. However, similar evolution of the Raman spectra with pressure was observed for barium hydride (BaH_2), where the ambient pressure phase, the orthorhombic cotunnite structure (*Pnma*), underwent a transition to the hexagonal Ni_2In-type phase ($P6_3/mmc$) at 1.6 GPa [18].

The Ni_2In-type and anticotunnite structures are closely related. In both structures, the walls of trigonal prisms of alkali atoms occupied by S atoms and sharing lateral edges are present. In the anticotunnite structure, these walls are puckered, whereas in the Ni_2In-type structure, they are straight [2,5]. Thus, the intensity changes observed in the diffraction patterns could be due to a continuous evolution between these two structures, as it is in the case of Cs_2S [5]. On the other hand, the Raman bands of anticotunnite phase located in the range 400–500 cm^{-1} exhibited broadening at pressures above 30 GPa, whereas the peak located at ≈ 250-260 cm^{-1}, which is the only one observed in the Ni_2In-type phase, remains relatively sharp at all pressures. Thus, we suppose that the anticotunnite-to-Ni_2In-type phase transition in Li_2S is of first order, as in Na_2S [2], and both phases coexist within the pressure range 30–45 GPa.

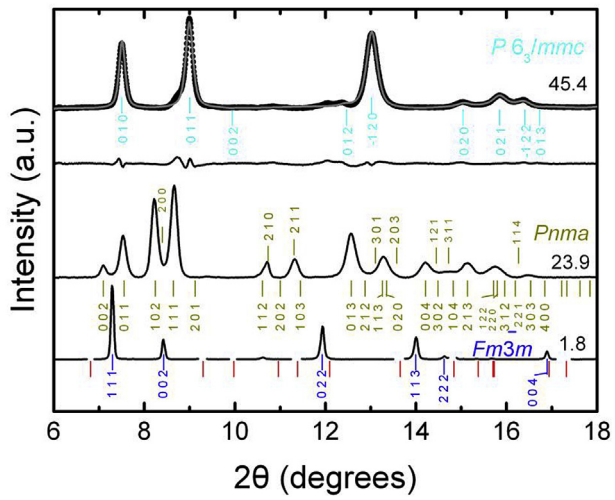

Fig. 4. Representative X-ray diffraction patterns of cubic antifluorite ($Fm\bar{3}m$), orthorhombic anticotunnite (*Pnma*) and hexagonal ($P6_3/mmc$, Ni_2In-type structure) phases of Li_2S. Red vertical bars denote reflections from the Al_2O_3 balls embedded in the Li_2S sample. Blue, dark yellow, and cyan vertical bars correspond to the Bragg reflections of low-pressure, cubic $Fm\bar{3}m$ phase; high pressure, orthorhombic *Pnma* phase; and high pressure, hexagonal $P6_3/mmc$ phase, respectively. Digits to the right show the corresponding pressure values in GPa. For the pattern at 45.4 GPa, structural refinement with hexagonal ($P6_3/mmc$) Ni_2In-type structure is shown: observed (symbols), calculated (solid gray line) and difference (solid black line). The difference line (given in the same scale) shows sufficiently good agreement between observed and calculated diffraction peaks positions. However, severe anisotropic peak broadening at high pressures and the presence of the remains of the *Pnma* phase lead to a rather poor profile, with a weighted *R*-agreement factor, $R_{wp} = 13.3\%$. (For interpretation of the references to colour in this figure legend, the reader is referred to the web version of this article.)

It should be noted that non-hydrostatic pressure conditions may be relevant in our experiments. Unfortunately, the chemical reactivity of the sample precludes the use of a pressure-transmitting medium; therefore, non-hydrostaticity may be the reason for the observed broad range of phase coexistence in the case of the anticotunnite-to-Ni_2In-type phase transition. Nevertheless, our observation of the transition to the Ni_2In-type structure in Li_2S is in good agreement with theoretical predictions [6,7] and the generalized phase diagram of alkali metal sulfides [5].

According to Raman spectroscopy data (Fig. 1), the Ni_2In-type phase remains stable up to the highest pressure of 64 GPa attained in our experiments. Up to this pressure, the sample remains transparent and colorless. Raman spectra recorded at pressure release (Fig. 1b) indicate that both the high-pressure phase transitions in Li_2S are reversible.

An interesting aspect of previous high-pressure studies on alkali metal sulfides was a comparison of the crystal structures of high-pressure phases of the sulfides, A_2S, with the cation arrays of the corresponding oxides, A_2SO_4 [2–5]. For all sulfides, the correlation between experimentally observed high-pressure structures and the cation subarrays of ambient-pressure polymorphs of the corresponding oxides was found, confirming the idea of formal equivalence between oxidation and pressure application [20]. For the Ni_2In-type structure of Li_2S, no related structure exists at ambient pressure in the corresponding sulfate Li_2SO_4, but at a pressure of 7 GPa the ε-phase of Li_2SO_4 adopts a structure isomorphic to the phase III of Na_2SO_4 [21], in which Na_2S subarrays are of the Ni_2In-type. Thus, also in the case of Li_2S, the correlation between its high-pressure structure and the cation subarray of its corresponding oxide can be established, allowing quantification of the pressure effect due to oxidation. Insertion of four oxygen atoms per Li_2S virtually produces the same effect as a pressure of ~25 GPa, which stabilizes the Ni_2In-type structure of Li_2S. This value is in accordance with a similar estimation for the Ni_2In-type structure of Na_2S, giving a value of 16 GPa [2].

Variation with pressure of the Li_2S lattice parameters and the unit cell volume is shown in Fig. 5. The relative change in the volume between orthorhombic and hexagonal phases at 31.9 GPa is 4.2%. The sequence of phase transitions observed under pressure for alkali metal sulfides (Li_2S, Na_2S, K_2S and Rb_2S), as well as the antifluorite-to-anticotunnite transformation reported by Lazicki et al. [9] for Li_2O, point to the systematic general phase transition sequence in alkali metal chalcogenides under high pressure.

The general sequence of the phase transitions in alkali metal chalcogenides and structurally related compounds at high pressures and/or elevated temperatures as proposed in previous reports [4,5,22,23] appears as follows: *anti*-$CaF_2 \rightarrow$ *anti*-$PbCl_2 \rightarrow Ni_2In \rightarrow$ *anti*-$TiSi_2$ $MgCu_2$-type (Laves phase). Development of the Zintl–Klemm concept described previously [22] has introduced a new general approach for explanation of pressure-induced phase transitions in various types of inorganic compounds,

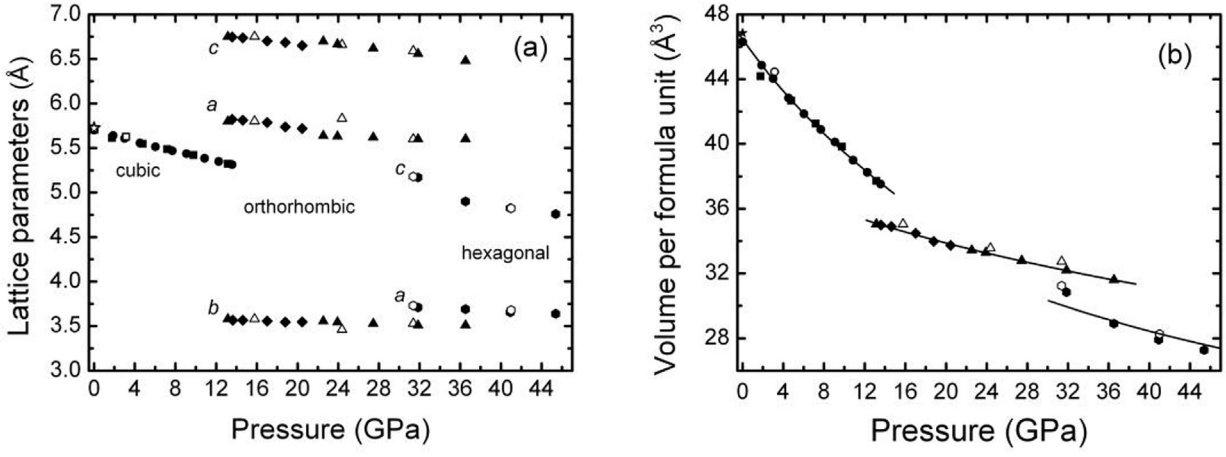

Fig. 5. Pressure dependences of the lattice parameters (a) and formula unit volume (b) of Li_2S. Circles and diamonds represent the data of [1] while squares ($Fm\bar{3}m$), triangles (*Pnma*) and hexagons ($P6_3/mmc$) represent the data obtained in the present study. Solid and open symbols denote data corresponding to increasing and decreasing pressure runs, respectively. Solid curves are Birch-Murnaghan equation of state fits to the experimental data. Star symbols denote the lattice parameter and volume values at ambient pressure from Ref. [19].

employing the ideas of 'pseudoatoms' and 'building skeletons' [22]. This novel approach allows one to predict structures of complex compounds from simple ones, e.g., AB building skeleton can be used for A_2B, AB_2, ABX_m compounds. According to the authors [22], this new method works only at a qualitative level. Its quantification requires intensive experimental and theoretical exploration of pressure-induced phase transitions of alkali metal oxides and chalcogenides similar to the recent investigations of alkaline earth fluorides in the 1–2 Mbar pressure range [24–27].

4. Conclusion

High-pressure Raman spectroscopy and X-ray powder diffraction studies of Li_2S reveal a sequence of reversible phase transitions from antifluorite to anticotunnite-type structure at ≈13 GPa, in agreement with previous high-pressure studies of Li_2S [1], and from anticotunnite-to-Ni_2In-type structure in the 30–45 GPa pressure range. The high-pressure phases of other alkali metal sulfides adopt the Ni_2In-type structure and the transition to this structure in Li_2S was predicted theoretically. Thus, presented results provide experimental evidence that all alkali sulfides undergo the same sequence (antifluorite-anticotunnite-Ni_2In type) of pressure-induced phase transitions. Recent observation of an antifluorite-to-anticotunnite transformation in Li_2O [9] reveals the general sequence of phase transitions in the alkali metal chalcogenides under high pressure.

Acknowledgements

We acknowledge the European Synchrotron Radiation Facility for granting the beam time and we would like to thank Dr. M. Hanfland for his assistance in using beamline ID-09.

References

[1] A. Grzechnik, A. Vegas, K. Syassen, I. Loa, M. Hanfland, M. Jansen, Reversible antifluorite to anticotunnite phase transition in Li_2S at high pressures, J. Solid State Chem. 154 (2000) 603–611.
[2] A. Vegas, A. Grzechnik, K. Syassen, I. Loa, M. Hanfland, M. Jansen, Reversible phase transitions in Na_2S under pressure: a comparison with the cation array in Na_2SO_4, Acta Crystallogr. Sect. B 57 (2001) 151–156.
[3] A. Vegas, A. Grzechnik, M. Hanfland, C. Mühle, M. Jansen, Antifluorite to Ni_2In-type phase transition in K_2S at high pressures, Solid State Sci. 4 (2002) 1077–1081.
[4] D. Santamaria-Perez, A. Vegas, C. Muehle, M. Jansen, High-pressure experimental study on Rb_2S: antifluorite to Ni2In-type phase transitions, Acta Crystallogr. Sect. B 67 (2011) 109–115.
[5] D. Santamaría-Pérez, A. Vegas, C. Muehle, M. Jansen, Structural behaviour of alkaline sulfides under compression: high-pressure experimental study on Cs_2S, J. Chem. Phys. 135 (2011) 054511.
[6] J.C. Schön, M.A.C. Wevers, M. Jansen, Prediction of high pressure phases in the systems Li_3N, Na_3N, $(Li,Na)_3N$, Li_2S and Na_2S, J. Mater. Chem. 11 (2001) 69–77.
[7] J.C. Schön, Ž. Čančarević, M. Jansen, Structure prediction of high-pressure phases for alkali metal sulfides, J. Chem. Phys. 121 (2004) 2289–2304.
[8] K. Kunc, I. Loa, A. Grzechnik, K. Syassen, Li_2O at high pressures: structural properties, phase-transition, and phonons, Phys. status solidi (b) 242 (2005) 1857–1863.
[9] A. Lazicki, C.S. Yoo, W.J. Evans, W.E. Pickett, Pressure-induced antifluorite-to-anticotunnite phase transition in lithium oxide, Phys. Rev. B 73 (2006) 184120.
[10] P. Demontis, M.L. Klein, R. LeSar, High-density structures and phase transition in an ionic model of H_2O ice, Phys. Rev. B 40 (1989) 2716–2718.
[11] P. Demontis, R. LeSar, M.L. Klein, New high-pressure phases of ice, Phys. Rev. Lett. 60 (1988) 2284–2287.
[12] A.P. Drozdov, M.I. Eremets, I.A. Troyan, V. Ksenofontov, S.I. Shylin, Conventional superconductivity at 203 kelvin at high pressures in the sulfur hydride system, Nature 525 (2015) 73–76.
[13] J.E. Hirsch, F. Marsiglio, Hole superconductivity in H_2S and other sulfides under high pressure, Phys. C Supercond. Appl. 511 (2015) 45–49.
[14] A.P. Hammersley, S.O. Svensson, M. Hanfland, A.N. Fitch, D. Hausermann, Two-dimensional detector software: from real detector to idealised image or two-theta scan, High Press. Res. 14 (1996) 235–248.
[15] F. Birch, Finite strain isotherm and velocities for single-crystal and polycrystalline NaCl at high pressures and 300 °K, J. Geophys. Res. Solid Earth 83 (1978) 1257–1268.
[16] R.W. Cheary, A. Coelho, A fundamental parameters approach to X-ray line-profile fitting, J. Appl. Crystallogr. 25 (1992) 109–121.
[17] P. Stephens, Phenomenological model of anisotropic peak broadening in powder diffraction, J. Appl. Crystallogr. 32 (1999) 281–289.
[18] J.S. Smith, S. Desgreniers, J.S. Tse, D.D. Klug, High-pressure phase transition observed in barium hydride, J. Appl. Phys. 102 (2007) 043520.
[19] F. Altorfer, W. Buhrer, I. Anderson, O. Scharpf, H. Bill, P.L. Carron, H.G. Smith, Structural Dynamic Properties of Li_2S, in: M. Balkanski, T. Takahashi, H.L. Tuller (Eds.), Solid State Ionics, Elsevier Science Publ B V, Amsterdam, 1992, pp. 325–330.
[20] A. Vegas, M. Jansen, Structural relationships between cations and alloys; an equivalence between oxidation and pressure, Acta Crystallogr. Sect. B–Struct. Sci. 58 (2002) 38–51.
[21] D.C. Parfitt, D.A. Keen, S. Hull, W.A. Crichton, M. Mezouar, M. Wilson, P.A. Madden, High-pressure forms of lithium sulphate: structural determination and computer simulation, Phys. Rev. B 72 (2005) 054121.
[22] A. Vegas, V. Garcıa-Baonza, Pseudoatoms and preferred skeletons in crystals, Acta Cryst. B63 (2007) 339–345.
[23] A. Vegas, Concurrent pathways in the phase transitions of alloys and oxides: towards an unified vision of inorganic solids, Struct. Bond. 138 (2011) 133–198. Berlin.
[24] S.M. Dorfman, F. Jiang, Z. Mao, et al., Phase transitions and equations of state of alkaline earth fluorides CaF_2, SrF_2, and BaF_2 to Mbar pressures, Phys. Rev. B 81 (2010) 174121.
[25] X. Wu, S. Qin, Z. Wu, First-principles study of structural stabilities, and electronic and optical properties of CaF_2 under high pressure, Phys. Rev. B 73 (2006) 134103.
[26] H. Ai-Min, Y. Xiao-Cui, L. Jie, et al., First-principles study of structural stabilities, electronic and optical properties of SrF_2 under high pressure, Chin. Phys. Lett. 26 (2009) 077103.
[27] H. Jiang, R. Pandey, C. Darrigan, M. Rerat, First-principles study of structural, electronic and optical properties of BaF_2 in its cubic, orthorhombic and hexagonal phases, J. Phys. Condens. Matter 15 (2003) 709–718.